

MEASUREMENT OF THE POSITRON TO ELECTRON RATIO IN THE COSMIC RAYS ABOVE 5 GeV

R. L. GOLDEN¹ AND S. J. STOCHAJ

Box 3-PAL, New Mexico State University, Las Cruces, NM 88003

S. A. STEPHENS

Tata Institute of Fundamental Research, Bombay 400 005, India

F. AVERSA, G. BARBIELLINI, M. BOEZIO, U. BRAVAR, A. COLAVITA, F. FRATNIK, P. SCHIAVON, A. VACCHI, AND N. ZAMPA
Dipartimento di Fisica dell'Università and Sezione Istituto Nazionale Fisica Nucleare di Trieste, Via A. Valerio 2, I-34147 Trieste, Italy

J. W. MITCHELL, J. F. ORMES, AND R. E. STREITMATTER

Code 661, NASA/Goddard Space Flight Center, Greenbelt, MD 20771

R. BELLOTTI, F. CAFAGNA, M. CASTELLANO, M. CIRCELLA, G. DE CATALDO, C. DE MARZO,
N. GIGLIETTO, B. MARANGELLI, A. RAINÒ, AND P. SPINELLI

Dipartimento di Fisica dell'Università and Sezione Istituto Nazionale Fisica Nucleare di Bari, Via Amendola 173, I-70126 Bari, Italy

M. BOCCIOLINI, N. FINETTI,² P. PAPINI, A. PEREGO, S. PICCARDI, AND P. SPILLANTINI

Dipartimento di Fisica dell'Università and Sezione Istituto Nazionale Fisica Nucleare di Firenze, Largo Enrico Fermi 2, I-50125 Firenze, Italy

G. BASINI, F. MASSIMO BRANCACCIO,³ AND M. RICCI

Laboratori Nazionali Istituto Nazionale Fisica Nucleare, Via Enrico Fermi 40, CP 13, I-00044 Frascati, Italy

M. T. BRUNETTI, A. CODINO, C. GRIMANI, AND M. MENICHELLI

Dipartimento di Fisica dell'Università and Sezione Istituto Nazionale Fisica Nucleare di Perugia, Via Pascoli, I-06100 Perugia, Italy

V. BIDOLI, M. CANDUSSO, M. CASOLINO, M. P. DE PASCALE, A. MORSELLI, P. PICOZZA, AND R. SPARVOLI

Dipartimento di Fisica dell'Università and Sezione Istituto Nazionale Fisica Nucleare di Roma, Tor Vergata, Via della Ricerca Scientifica 1, I-00133 Roma, Italy

AND

M. HOF, W. MENN, AND M. SIMON

Siegen University, 57068, Siegen, Germany

Received 1995 August 3; accepted 1995 November 17

ABSTRACT

As part of a series of experiments to search for antimatter in cosmic rays, the New Mexico State University balloon-borne magnet spectrometer was configured for a flight to study positrons. Two completely new instruments, a transition radiation detector and a silicon-tungsten imaging calorimeter, were added to the magnet spectrometer. These two detectors provided a proton rejection factor better than 3×10^4 . This instrument was flown from Fort Sumner, New Mexico, at an average depth of 4.5 g cm^{-2} of residual atmosphere for a period of 25 hr. We report here the measured fraction of positrons $e^+/(e^+ + e^-)$ from ~ 5 to 60 GeV at the top of the atmosphere. Our measurements do not show any compelling evidence for an increase in this ratio with energy, and our results are consistent with a constant fraction of 0.078 ± 0.016 over the entire energy region.

Subject headings: cosmic rays — elementary particles

1. INTRODUCTION

Although the electron component constitutes less than 1% of the cosmic rays, it plays an important role in understanding the propagation of cosmic rays in the Galaxy. This is because electrons undergo severe energy loss through inverse-Compton scattering with the ambient photons and synchrotron radiation in the magnetic field. The astrophysical importance of positrons stems from their intimate relationship with the radio and gamma-ray background in the Galaxy. The observed positron-to-electron ratio of $\sim 10\%$ shows that positrons are indeed a rare component of cosmic rays. Furthermore, previous observations have shown that their fraction appears to increase above 5 GeV (see, e.g., Golden et al. 1987, 1994;

Muller & Tang 1987). This increase cannot be explained by the known propagation theories, but rather it requires a new source of positrons. Several theories have explored the idea of primary sources for positrons. At the same time, attempts have been made to confirm these positron observations with improved detector systems. The unambiguous detection of positrons is difficult because of the vast background of protons. In this Letter we briefly describe a recent measurement of the positron fraction above 5 GeV using a balloon-borne magnet spectrometer with an improved detector systems.

2. DETECTOR SYSTEM

Figure 1 shows the schematic diagram of the TS93 apparatus that was flown by balloon from Fort Sumner on 1993 September 8 at a constant altitude of 36 km for 25 hr. This instrument consisted of the following detector elements.

1. A superconducting magnet spectrometer with multiwire proportional chambers (MWPC) and drift chambers (Golden

¹ Deceased.

² Now at Dipartimento di Fisica dell'Università and Sezione INFN di Perugia, Via Pascoli, I-06100 Perugia, Italy.

³ Now at Sezione INFN di Firenze, Largo Enrico Fermi 2, I-50125 Firenze, Italy.

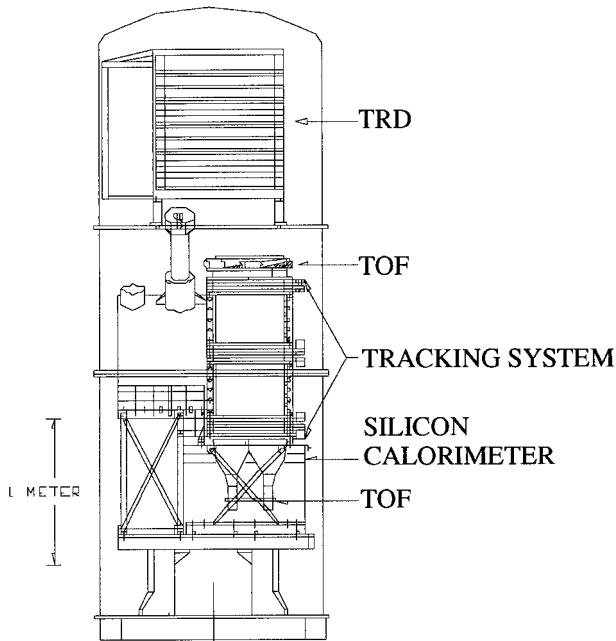


FIG. 1.—Schematic diagram of the TS93 apparatus

et al. 1991; Hof et al. 1994) was used to measure the curvature of the particles with an estimated average maximum detectable rigidity of $200 \text{ GV } c^{-1}$.

2. A transition radiation detector (TRD) was positioned above the spectrometer. The TRD consisted of 10 layers of carbon fiber radiators, each followed by a MWPC. The signal from each wire of the MWPC was analyzed with cluster counting capability (Barbarito et al. 1992; Bellotti et al. 1992, 1993). The TRD was used as a threshold detector for the estimate of the particle velocity (Lorentz factor).

3. A set of plastic scintillators was placed at the upper and lower extremes of the spectrometer, providing the basic trigger for the experiment. Time-of-flight (TOF) information from these paddles was used to distinguish upward-moving particles from downward with a resolution of 400 ps over 1.4 m flight path. Pulse height information was used as a measure of the particle's ionization losses.

4. A silicon-tungsten imaging calorimeter was kept at the bottom of the detector system. This consisted of five sets of silicon planes, giving both x - and y -coordinates readouts. Each set of readout planes was interleaved with a plane of tungsten, one radiation length thick (Aversa et al. 1993, 1995).

3. DATA ANALYSIS

We required a well-defined single track in the spectrometer with a good momentum resolution, characterized by acceptable chi-squares and small uncertainty in deflection. Then, using the ionization measurements from the TOF scintillators, we identified minimum ionizing particles with $I < 3.0I_0$, where I_0 is the most probable scintillator output for a minimum ionizing singly charged particle.

Downward-moving events with negative curvature were selected, and those having electromagnetic shower in the calorimeter were classified as e^- events. These events contained a very small fraction of locally produced pions at very low energies. We observed a total of 1033 electrons above 1 GeV, of which 317 were in the 6–50 GeV range.

The selected e^- events were then used to develop selection criteria for the calorimeter to define a pure electromagnetic cascade. These criteria were also studied using Monte Carlo simulations (Brun et al. 1994), the results of which were previously tested using accelerator data (Boccolini et al. 1993a, 1993b). They include longitudinal and lateral profiles of pure electromagnetic cascades, total deposited energy, and the energy flow along a well-defined core of the cascade. The loss of events resulting from the application of these criteria was then determined by using e^- events, which were selected by the TRD. It was found that the efficiency of the calorimeter, with these selection criteria, was independent of energy in the range 1–50 GeV and was 0.79 ± 0.02 . When these cuts were imposed on the positively charged particles, we achieved a mean proton rejection factor of 455 ± 21 above 4 GeV that was found to be nearly independent of energy from 4 to 50 GeV. The rejection factor slowly decreased below 4 GeV to $\sim 178 \pm 24$ at 1.5 GeV. However, the observed ratio of protons to positrons below the geomagnetic cutoff also decreased by a factor of ~ 25 over this same energy interval. Therefore, the contamination by particles not accompanied by an electromagnetic cascade remains very small over the entire energy range from 1 to 50 GeV.

The TRD selection criteria were based on the sum of the hits in the MWPC along the track and the number of such planes, activated during the passage of the event. These criteria were earlier studied using accelerator beams (Barbarito et al. 1992; Bellotti et al. 1992, 1993). By applying these criteria to the e^- events, which were selected by the calorimeter, we estimated the efficiency of the TRD to be 0.69 ± 0.02 above 3 GeV. Below 3 GeV, this efficiency dropped to 0.60 ± 0.03 . By applying these criteria to positively charged particles, we found that the proton rejection factor by the TRD was 76.9 ± 2.4 . It may be noted that the velocity measurements using TOF scintillators also provided an effective rejection of protons of rigidity less than $2 \text{ GV } c^{-1}$.

4. RESULTS

We have shown in Table 1 the observed number of e^- and e^+ events that passed both the calorimeter and TRD cuts. The energy intervals shown were measured at the spectrometer. Since the proton rejection power of the instrument was not 100%, we expect that the selected positron sample would contain a few proton events. In order to estimate this contamination, we first constructed the proton spectrum using the flight data. The observed proton spectrum was then divided by the proton rejection factor to estimate this proton contamination. In Table 1 the estimated residual protons are shown in parentheses along with the positron number. As we do not have the absolute efficiencies resulting from the spectrometer cuts used in this analysis, we estimated the atmospheric secondaries in the following manner. We first constructed the differential spectra for both electrons and positrons from 1 to 50 GeV. These spectra were corrected for the TRD efficiency and then propagated to the top of the payload through the material above the spectrometer using the bremsstrahlung process. These extrapolated flux values are plotted as a function of energy in Figure 2. One can clearly notice from this figure the effect of the geomagnetic cutoff below ~ 6 GeV. The total electron spectrum above 6 GeV is consistent with a simple power law having a spectral index of -3.3 , as obtained from earlier measurements (Golden et al. 1984, 1987). The

TABLE 1
SUMMARY OF ELECTRON-POSITRON RESULTS

ENERGY BIN AT SPECTROMETER (GeV) (1)	OBSERVED NUMBER OF EVENTS ^a		MEDIAN ENERGY AT TOA (4)	CORRECTED NUMBER AT TOA		$[e^+/(e^+ + e^-)]$ (7)
	e^- (2)	e^+ (3)		e^- (5)	e^+ (6)	
4.0–5.0.....	109	14 (0.9)	5.71	129.0 ± 12.6	11.50 ± 4.0	0.082 ± 0.027
5.0–7.0.....	165	17 (1.5)	7.49	163.6 ± 13.0	11.56 ± 3.54	0.066 ± 0.019
7.0–11.....	97	11 (1.3)	10.8	78.4 ± 8.08	6.57 ± 2.47	0.077 ± 0.028
11–50.....	56	10 (1.3)	22.0	40.5 ± 5.70	5.01 ± 2.25	0.110 ± 0.046

^a The numbers shown in the parentheses are the residual proton contamination.

marked increase at low energies is due to secondary electrons produced by hadron interactions in the atmosphere. This part of the spectrum was used as a guide to correct for the secondaries produced in the overlying atmosphere above the cutoff energy.

The solid and dashed curves shown in Figure 2 are, respectively, the e^+ and e^- spectra of secondary electrons produced by the interactions of cosmic-ray nuclei in the overlying atmosphere (Stephens 1981). This expected secondary positron spectrum was normalized to the observed spectrum below 3 GeV. We noticed that the secondary spectra are not a simple power-law spectra over the entire energy region. This is due to the varying contribution from the decay of charged and neutral pions in the atmosphere. It can also be seen that while the e^+ spectrum below the geomagnetic cutoff appears to be dominated by the secondaries, the e^- spectrum is not. In order to understand this difference, we examined the effect of the propagation of primary electrons in the following manner. We assumed the primary e^- and e^+ above 6 GeV to have the same spectra as in Figure 2 at the top of the atmosphere (TOA). To get the spectral shape below this energy, we normalized at 6 GeV the observed rigidity spectrum of helium nuclei, which was obtained from this experiment. This procedure provides the best method to take care of the effect of geomagnetic cutoff and penumbral bands. We then propagated these spectra from the top of the atmosphere to the float altitude by solving simultaneously the cascade equations, which describe the propagation of all the electromagnetic components, namely, primary e^- , e^+ and secondary gamma rays. Note that these gamma rays are produced by the electrons through the bremsstrahlung process in the atmosphere. It was found that the noticeable difference between the observed e^- spectrum below the cutoff and the secondary spectrum (dashed curve in Fig. 2) can be explained as due to the slowing down of the primary electrons. Because of the small atmospheric depth at which the experiment was conducted, we also found from this calculation that the contribution to e^+ from the cascading of the dominant e^- component was very small compared to the secondaries produced by hadron interactions. Thus we are very confident that the procedure adopted here is very reliable.

We have subtracted the expected number of secondary e^- and e^+ in the extrapolated energy bins at the top of the payload. While doing this, we included in the secondary correction an uncertainty equivalent to 1σ of the observed e^+ flux values over the energy region where the normalization was made. The remainder of the e^- , e^+ , and calculated gamma rays that were at the float altitude and above the geomagnetic cutoff were propagated backward to the top of the atmosphere by simultaneously solving the cascade equations. In Table 1, we show the median energy and the corrected number of e^-

and e^+ in columns (4) to (6), respectively, at the TOA. The errors include not only the statistics, but also those discussed above. It may be pointed out that the extrapolated energy bins at the TOA are based on the mean radiation loss over the total amount of ~ 0.24 radiation length of matter above the spectrometer, which includes both the material in the instrument and the atmosphere. Column (7) in Table 1 gives the observed fraction of e^+ at the top of the atmosphere. The values that we have obtained are nearly constant over the first three intervals from 5 to 14 GeV, producing a mean value of 0.074 ± 0.016 . The last value, although higher, is consistent with those at low-energy bins within 1σ . Therefore, combining all the bins, we obtained a value of 0.078 ± 0.016 for the fraction of positrons among the electron component of cosmic rays in the energy region from 5 to 63 GeV.

Figure 3 shows the fraction of positrons as observed by us along with the other existing published data as a function of energy from ~ 500 MeV to 60 GeV (Fanselow et al. 1969; Buffington et al. 1975; Muller & Tang 1987; Golden et al. 1987, 1994; Barwick et al. 1995). It can be noted that the present results are in agreement with the results obtained earlier using the same magnet spectrometer with different detector systems. It can also be seen that, except for the high-energy data points from Buffington et al. (1975) and Muller & Tang (1987), there

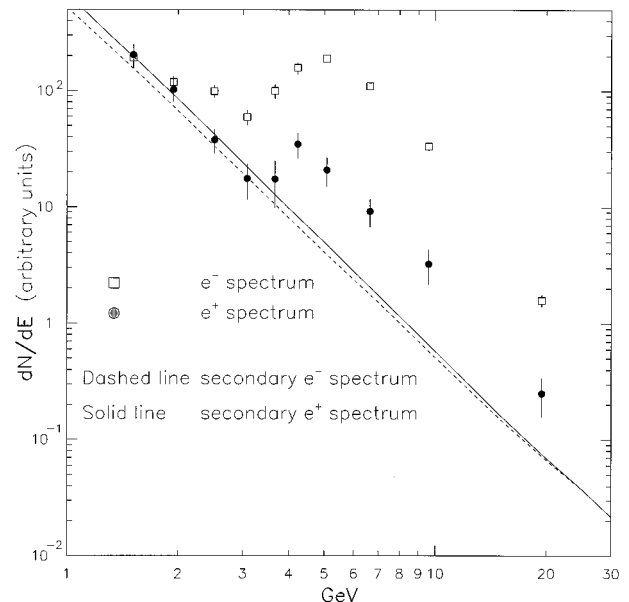


Fig. 2.—Extrapolated positron and electron spectra at the top of the payload. The solid and dashed curves are the secondary spectra produced by the interactions of cosmic-ray nuclei in the atmosphere (Stephens 1981).

is no compelling evidence for e^+ fraction to increase with energy above 10 GeV, and the data points suggest a fraction that is independent of energy, within errors, over the entire energy range of the measurement. We have also shown in this figure the expected fraction of e^+ from simple leaky box model (Protheroe 1992) and the recent observations are not inconsistent with the predictions. It may be noted that the theoretical prediction is indeed an underestimation because the path length used for the matter traversed by cosmic rays in the Galaxy was smaller than what is known today. It may be pointed out that our results do not exhibit the trend shown by Barwick et al. (1995), in which the positron fraction decreases with energy. However, the errors associated with the high-energy measurements in both experiments are too large to claim a significant difference. It is very important to improve the detection efficiency of the instrument and to extend the measurements to lower and higher energies in a single experiment.

This work was supported by NASA grant NAGW-110, The Istituto Nazionale di Fisica Nucleare, Italy, the Agenzia Spaziale Italiana and DARA and DFG in Germany. We wish to thank the National Scientific Balloon Facility and the NSBF launch crew that served at Fort Sumner.

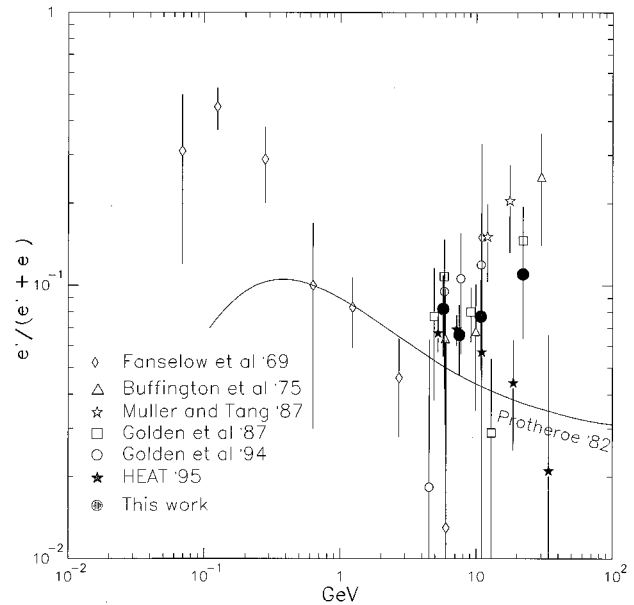


FIG. 3.—Positron fraction, $[e^+/(e^+ + e^-)]$, as observed in this experiment compared with other published data and the simple leaky box model.

REFERENCES

- Aversa, F., et al. 1993, Nucl. Instrum. Meth., A334, 589
 ———. 1995, Nucl. Instrum. Meth., A360, 17
 Barbarito, E., et al. 1992, Nucl. Instr. Meth., A313, 295
 Barwick, S. W., et al. 1995, Phys. Rev. Lett., 75, 390
 Bellotti, R., et al. 1992, Nucl. Instrum. Meth., A323, 295
 ———. 1993, in Proc. 23d Internat. Cosmic Ray Conf. (Calgary), 635
 Bocciolini, M., et al. 1993a, Nucl. Instrum. Meth., A333, 77
 ———. 1993b, Nucl. Phys., 32, 77
 Brun, R., et al. 1994, Detector Description and Simulation Tool, CERN program library
 Buffington, A., Orth, C. D., & Smooth, G. F. 1975, ApJ, 199, 669
 Fanelow, J. L., Hartman, R. C., Hildebrand, R. H., & Meyer, P. 1969, ApJ, 158, 771
 Golden, R. L., Mauger, B. G., Badhwar, G. D., Daniel, R. R., Lacy, J. L., Stephens, S. A., & Zipse, J. E. 1984, ApJ, 287, 622
 Golden, R. L., Stephens, S. A., Mauger, B. G., Badhwar, G. D., Daniel, R. R., Horan, S., Lacy, J. L., & Zipse, J. E. 1987, A&A, 188, 145
 ———. 1991, Nucl. Instrum. Meth., A306, 366
 ———. 1994, ApJ, 436, 769
 Hof, M., et al. 1994, Nucl. Instrum. Meth., A345, 561
 Muller, D., & Tang, K. K. 1987, ApJ, 312, 183
 Protheroe, R. J. 1982, ApJ, 254, 391
 Stephens, S. A. 1981, Proc. 17th Internat. Cosmic Ray Conf. (Paris), Vol. 4, 282